VELOCITY AMBIGUITY MITIGATION OF OFF-GRID RANGE MIGRATING TARGETS VIA BAYESIAN SPARSE RECOVERY

Marie Lasserre, Stéphanie Bidon

ISAE/University of Toulouse, Toulouse, France

François Le Chevalier

MS^3, Delft University of Technology, Delft, The Netherlands

ABSTRACT

Within the scope of sparse signal representation, we consider the problem of velocity ambiguity mitigation for wideband radar signal. We present a Bayesian robust algorithm based on a new sparsifying dictionary suited for range-migrating targets possibly straddling range-velocity bins. Numerical simulations on experimental data demonstrate the ability of the proposed algorithm in mitigating velocity ambiguity.

***Index Terms*—** Bayesian estimation, Sparse signal representations (SSR), wideband radar

1. INTRODUCTION

A radar system transmitting a train of pulses at constant pulse repetition frequency (PRF) suffers from two types of ambiguities: range ambiguities (if the PRF is too high) or velocity ambiguities (if the PRF is too low) [1]. Moreover, one cannot increase the ambiguous range without decreasing the ambiguous velocity, and reciprocally. Wideband radar systems offer an alternative to the problem of ambiguity removal [2, 3]. More precisely, if we assume that a low PRF is used, there are no range ambiguities but many velocity ambiguities. Additionally, using a wide instantaneous bandwidth improves range resolution, so that fast moving targets are likely to migrate during the coherent processing interval (CPI) leading to range-velocity coupling. Unlike conventional Doppler phase measurement, this range walk phenomenon can give unambiguous velocity measurement.

Sparse signal representation (SSR) can be of particular interest when trying to remove velocity ambiguities since it allows the estimation of a sidelobe-less signal of interest (SOI) [4],[5, chap.5]. SSR relies on a *sparsifying dictionary* that results from a discretization of the range and velocity dimensions (in the case of this bi-dimensional problem) and hence define some analysis grid. In [6] an SSR algorithm was developed within this framework and proven to mitigate velocity ambiguities, provided that target's features belong to the analysis grid. Otherwise, as mentioned in [7, 8, 9, 10] a problem of *grid-mismatch* might arise and disrupt velocity ambiguity mitigation. In [7, 8] two SSR algorithms robustified towards grid mismatch are presented in the case of narrowband radar signal where 1D and 2D Fourier analysis grids are used respectively (resp.). Here, the novelty lies into the new sparsifying dictionary that takes into account range migration, and the corresponding estimation scheme; the algorithm is developed within a Bayesian framework.

The remaining of the paper is organized as follows. First, the wideband signal model is described in Section 2. Then, the proposed Bayesian hierarchical model and the associated estimation scheme are presented in Section 3 and 4 resp. The proposed algorithm is finally evaluated on experimental data in Section 5.

2. SIGNAL MODEL

The signal model used to describe migrating targets has been introduced in [6]. In this paper, a row-vectorized version of this model is used

$$\boldsymbol{y} = \sum_{n=1}^{N} \alpha_n \boldsymbol{a}_n + \boldsymbol{n} \tag{1}$$

where each vector has a length KM, K being the number of subbands and M the number of pulses corresponding to the received samples gathered in vector $\boldsymbol{y}$. $\boldsymbol{n}$ is the noise vector; α_n, $\boldsymbol{a}_n$ and N represent the complex amplitude and signature of the nth scatterer, and the total number of scatterers in the scene. The scatterer signature $\boldsymbol{a}$ involved in (1) is the product of a conventional 2D-cisoid with *cross-coupling terms* that model the range migration, i.e.,

$$[\boldsymbol{a}]_{m+kM} = e^{j2\pi\left(-\tau_0 \frac{B}{K}k + \frac{2vf_c}{c}T_r m\left(1+\frac{B}{Kf_c}k\right)\right)} \tag{2}$$

where f_c is the carrier frequency, B the bandwidth, T_r the pulse repetition interval (PRI); τ_0 is the initial round-trip delay of the scatterer and v its radial velocity. $f_d \triangleq 2vf_cT_r/c$ is the normalized Doppler frequency of the scatterer, while $f_r \triangleq \tau_0 B/K$ represents its normalized range frequency. In

The work of M. Lasserre and S. Bidon is supported by the Direction Générale de l'Armement via a DGA-MRIS scholarship.

the following equations, the fractional bandwith per subband $\mu = B/(Kf_c)$ is used.

Within the scope of SSR methods, the signal $\boldsymbol{y}$ is reformulated as

$$\boldsymbol{y} = \boldsymbol{H}\boldsymbol{x} + \boldsymbol{n} \tag{3}$$

where $\boldsymbol{x}$ is a sparse vector that represents the targets amplitude and $\boldsymbol{H}$ is a $KM \times \bar{K}\bar{M}$ sparsifying dictionary that stems from a discretization of the range and velocity dimensions, $\bar{K}\bar{M}$ being the dimensions of reconstruction of the scene. Then, using (2) the $\bar{i}$-th column of the dictionary $\boldsymbol{H}$ is expressed as

$$[\boldsymbol{h}_{\bar{i}}]_i = \frac{1}{\sqrt{KM}} \exp\{-j2\pi f_{r\bar{i}} k\} \exp\{j2\pi f_{d\bar{i}}(1+\mu k)m\}$$

where $f_{r\bar{i}}$ and $f_{d\bar{i}}$ are the normalized range and Doppler frequencies from the range and velocity analysis grids. The table indices k, m, i and $\bar{k}$, $\bar{m}$, $\bar{i}$ used to index the sparsifying dictionary $\boldsymbol{H}$ are related as $i = m + kM$ ($k \in \{0, K-1\}$, $m \in \{0, M-1\}$) and similarly for $\bar{i}$, $\bar{k}$, $\bar{m}$.

The range analysis grid is divided into $\bar{K}$ bins with a possible zero-padding factor, so that $\bar{K} = n_{zp}^r K$. Then, the normalized range Doppler frequency $f_{r\bar{i}}$ of a scatterer located at the $\bar{k}$-th range bin is expressed as $f_{r\bar{i}} = \bar{k}/\bar{K}$.

In order to mitigate velocity ambiguity, the range-velocity map is unfolded with a factor of n_{va} on the velocity axis. Taking into account positive and negative velocities leads us to consider a velocity analysis grid that goes from $-n_{va}v_a/2$ to $n_{va}v_a/2$, where $v_a = c/(2f_cT_r)$ is the ambiguous velocity.

This grid is divided into $\bar{M}$ bins with $\bar{M} = n_{zp}^v n_{va} M$ where n_{zp}^v represents the zero-padding factor per velocity ambiguity. The normalized Doppler frequency is then $f_{d\bar{i}} = n_{va}\bar{m}'/\bar{M}$ where (assuming $\bar{M}$ is even) $\bar{m}' = \bar{m}$ if $\bar{m} \in \{0, ..., \bar{M}/2-1\}$; $\bar{m}' = \bar{m} - \bar{M}$ if $\bar{m} \in \{\bar{M}/2, ..., \bar{M}-1\}$.

As explained in [7, 8], the range and velocity of the targets present in the radar scene does not necessarily coincide with that of the sparsifying dictionary $\boldsymbol{H}$. Following the approach proposed in [8] two mismatch vectors $(\boldsymbol{\varepsilon}^v, \boldsymbol{\varepsilon}^r)$ are introduced to address the mismatch problem on the velocity and range axis resp. They parametrize the sparsifying dictionary $\boldsymbol{H}$ such that

$$f_{d\bar{i}} = \frac{\bar{m}' + \varepsilon_{\bar{i}}^v}{\bar{M}} n_{va}, \qquad f_{r\bar{i}} = \frac{\bar{k} + \varepsilon_{\bar{i}}^r}{\bar{K}}. \tag{4}$$

Generally speaking, the problem (3) is ill-posed because $\bar{K}\bar{M} >> KM$ (especially when the range-velocity maps are unfolded, i.e., $n_{va} > 1$); in this paper, the problem is regularized using a Bayesian approach.

3. HIERARCHICAL BAYESIAN MODEL

A Bayesian framework is set up in order to estimate the parameters of interest $\boldsymbol{x}$ and $(\boldsymbol{\varepsilon}^v, \boldsymbol{\varepsilon}^r)$. The hierarchical Bayesian model adopted is that of [8] so it is briefly recalled in this section. However, note that the sparsifying dictionary in case of migrating targets will demand a new method for the sampling of the mismatch parameters $(\boldsymbol{\varepsilon}^v, \boldsymbol{\varepsilon}^r)$.

3.1. Likelihood

The noise vector $\boldsymbol{n}$ is assumed white and distributed following a centered Gaussian distribution with power σ^2. The likelihood function is then expressed as

$$f(\boldsymbol{y}|\sigma^2, \boldsymbol{x}, \boldsymbol{\varepsilon}^v, \boldsymbol{\varepsilon}^r) = \frac{\exp\left\{-\frac{||\boldsymbol{y} - \boldsymbol{H}(\boldsymbol{\varepsilon}^v, \boldsymbol{\varepsilon}^r)\boldsymbol{x}||^2}{\sigma^2}\right\}}{(\pi\sigma^2)^{KM}}. \tag{5}$$

3.2. Prior model

3.1.1) Target amplitude vector $\boldsymbol{x}$

The elements $x_{\bar{i}} \triangleq [\boldsymbol{x}]_{\bar{i}}$ of the amplitude vector are assumed independent and identically distributed (iid) according to the following mixed type probability density function (pdf)

$$\pi(x_{\bar{i}}|w, \sigma_x^2) = (1-w)\delta(|x_{\bar{i}}|) + w\frac{1}{\pi\sigma_x^2} \exp\left\{-\frac{|x_{\bar{i}}|^2}{\sigma_x^2}\right\}. \tag{6}$$

The prior (6) is denoted as $x_{\bar{i}}|w, \sigma_x^2 \sim \mathcal{B}er\mathcal{CN}\left(w, 0, \sigma_x^2\right)$. It promotes the sparsity of the radar scene, while decorrelating sparsity level and target power via its mixed-type structure.

3.1.2) Noise power σ^2

An inverse-gamma prior is chosen for the white noise power σ^2; it is denoted $\mathcal{IG}(\gamma_0, \gamma_1)$ and can be expressed as

$$\pi(\sigma^2|\gamma_0, \gamma_1) \propto \frac{e^{-\gamma_1/\sigma^2}}{(\sigma^2)^{\gamma_0+1}} \mathbb{I}_{[0,+\infty)}(\sigma^2) \tag{7}$$

where γ_0, γ_1 are resp. the shape and scale parameters.

3.1.3) Target signal power σ_x^2

Similarly to σ^2, an inverse-gamma prior is chosen for the target signal power σ_x^2 and is denoted as $\sigma_x^2|\beta_0, \beta_1 \sim \mathcal{IG}(\beta_0, \beta_1)$.

3.1.4) Level of occupancy w

If no information is available about the sparsity level of the target scene, a convenient prior is a uniform pdf over the interval $[0, 1]$, i.e., $w \sim \mathcal{U}_{[0,1]}$.

3.1.5) Grid errors $(\boldsymbol{\varepsilon}^v, \boldsymbol{\varepsilon}^r)$

The joint prior pdf of the grid error in the $\bar{i}$th analysis bin $(\varepsilon_{\bar{i}}^v, \varepsilon_{\bar{i}}^r)$ is chosen conditioned to the magnitude of $x_{\bar{i}}$; we consider that the $(\varepsilon_{\bar{i}}^v, \varepsilon_{\bar{i}}^r|x_{\bar{i}})$ are iid with conditional joint pdf

$$\pi(\varepsilon_{\bar{i}}^v, \varepsilon_{\bar{i}}^r|x_{\bar{i}} = 0) = \delta(\varepsilon_{\bar{i}}^v)\delta(\varepsilon_{\bar{i}}^r) \tag{8a}$$

$$\pi(\varepsilon_{\bar{i}}^v, \varepsilon_{\bar{i}}^r|x_{\bar{i}} \neq 0) = \mathbb{I}_{[-0.5,0.5]}(\varepsilon_{\bar{i}}^v)\mathbb{I}_{[-0.5,0.5]}(\varepsilon_{\bar{i}}^r) \tag{8b}$$

where $\mathbb{I}_A(.)$ is the indicator function of the set A.

4. BAYESIAN ESTIMATION

We propose an estimation scheme of the target scene via the parameters of interest $\boldsymbol{x}, (\boldsymbol{\varepsilon}^v, \boldsymbol{\varepsilon}^r)$ based on the Bayesian hierarchical model described in Section 3. More precisely, our objective is to obtain the minimum mean square error (MMSE) estimators of $\boldsymbol{x}$ and $(\boldsymbol{\varepsilon}^v, \boldsymbol{\varepsilon}^r)$

$$\hat{\boldsymbol{x}}_{\text{MMSE}} = \int \boldsymbol{x} f(\boldsymbol{x}|\boldsymbol{y}) d\boldsymbol{x}, \tag{9a}$$

$$\left(\hat{\boldsymbol{\varepsilon}^v}, \hat{\boldsymbol{\varepsilon}^r}\right)_{\text{MMSE}} = \int (\boldsymbol{\varepsilon}^v, \boldsymbol{\varepsilon}^r) f(\boldsymbol{\varepsilon}^v, \boldsymbol{\varepsilon}^r|\boldsymbol{y}) d\boldsymbol{\varepsilon}^v d\boldsymbol{\varepsilon}^r. \tag{9b}$$

However, (9) seems intractable to derive analytically, so a Monte-Carlo Markov Chain (MCMC) is implemented [11]. More specifically, an hybrid Gibbs sampler [11, chap.10] is used, which simulates iteratively samples ${\theta_i}^{(t)}$ according to their conditional posterior distribution $f(\theta_i|\boldsymbol{y}, \boldsymbol{\theta}_{-i})$ where $\boldsymbol{\theta} = \left[\sigma^2, {\boldsymbol{\varepsilon}^v}^T, {\boldsymbol{\varepsilon}^r}^T, \boldsymbol{x}^T, w, \sigma_x^2\right]^T$ and $\boldsymbol{\theta}_{-i}$ is the vector $\boldsymbol{\theta}$ whose ith element has been removed. After a burn in time N_{bi}, the samples are distributed according to their posterior distribution $f(\theta_i|\boldsymbol{y})$. When enough samples are acquired (N_r), the MMSE estimators can be built empirically as

$$\hat{\theta}_{i\text{MMSE}} = N_r^{-1} \sum_{t=1}^{N_r} {\theta_i}^{(t+N_{bi})}. \tag{10}$$

The conditional posterior distributions are obtained from the joint posterior pdf of $\sigma^2, \boldsymbol{x}, \boldsymbol{\varepsilon}^v, \boldsymbol{\varepsilon}^r, w, \sigma_x^2|\boldsymbol{y}$. In particular, vectors $\boldsymbol{x}$ and $(\boldsymbol{\varepsilon}^v, \boldsymbol{\varepsilon}^r)$ are sampled element-wise following the conditional posterior distributions of $x_{\bar{i}}$ and $(\varepsilon_{\bar{i}}^v, \varepsilon_{\bar{i}}^r)$ that are derived from the conditional joint posterior distribution

$$\begin{aligned} &f(\varepsilon_{\bar{i}}^v, \varepsilon_{\bar{i}}^r, x_{\bar{i}}|\boldsymbol{y}, \boldsymbol{\varepsilon}_{-\bar{i}}^v, \boldsymbol{\varepsilon}_{-\bar{i}}^r, \boldsymbol{x}_{-\bar{i}}, \sigma^2, w, \sigma_x^2) \\ &\propto \exp\left\{ \frac{-\left[|x_{\bar{i}}|^2 ||\boldsymbol{h}_{\bar{i}}(\varepsilon_{\bar{i}}^v, \varepsilon_{\bar{i}}^r)||^2 - 2\,\mathcal{R}\text{e}\left\{x_{\bar{i}}^* \boldsymbol{h}_{\bar{i}}(\varepsilon_{\bar{i}}^v, \varepsilon_{\bar{i}}^r)^H \boldsymbol{e}_{\bar{i}}\right\}\right]}{\sigma^2} \right\} \\ &\quad \times \pi(x_{\bar{i}}|w, \sigma_x^2) \pi(\varepsilon_{\bar{i}}^v, \varepsilon_{\bar{i}}^r|x_{\bar{i}}) \end{aligned} \tag{11}$$

where we used (5) along with the fact that $\boldsymbol{y} - \boldsymbol{H}(\boldsymbol{\varepsilon}^v, \boldsymbol{\varepsilon}^r)\boldsymbol{x} = \boldsymbol{e}_{\bar{i}} - \boldsymbol{h}_{\bar{i}} x_{\bar{i}}$ with $\boldsymbol{e}_{\bar{i}} = \boldsymbol{y} - \sum_{l \neq \bar{i}} \boldsymbol{h}_l(\varepsilon_l^v, \varepsilon_l^r) x_l$.

4.1. Sampling of $\boldsymbol{x}$, σ^2, w, and σ_x^2

Following [7], $\boldsymbol{x}$ is sampled element-wise; the $\bar{i}$th element of $\boldsymbol{x}$ follows the distribution $\mathcal{B}er\mathcal{CN}\left(w_{\bar{i}}, \mu_{\bar{i}}, \eta_{\bar{i}}^2\right)$ with

$$\eta_{\bar{i}}^2 = \left(\sigma^{-2} + \sigma_x^{-2} ||\boldsymbol{h}_{\bar{i}}(\varepsilon_{\bar{i}}^v, \varepsilon_{\bar{i}}^r)||^2\right)^{-1} \tag{12a}$$

$$\mu_{\bar{i}} = \sigma^{-2} \eta_{\bar{i}}^2 \boldsymbol{h}_{\bar{i}}(\varepsilon_{\bar{i}}^v, \varepsilon_{\bar{i}}^r)^H \boldsymbol{e}_{\bar{i}} \tag{12b}$$

$$w_{\bar{i}} = \frac{w}{(1-w)\sigma_x^2 \eta_{\bar{i}}^{-2} \exp\left\{-\eta_{\bar{i}}^{-2} |\mu_{\bar{i}}|^2\right\} + w}. \tag{12c}$$

Note that with the sparsifying dictionary $\boldsymbol{H}$ adopted $||\boldsymbol{h}_{\bar{i}}(\varepsilon_{\bar{i}}^v, \varepsilon_{\bar{i}}^r)||^2 = 1$.

The conditional posterior distributions of σ^2, σ_x^2 and w are given by

$$\begin{aligned} \sigma^2|\boldsymbol{y}, \boldsymbol{x}, \boldsymbol{\varepsilon}^v, \boldsymbol{\varepsilon}^r &\sim \mathcal{IG}\left(\gamma_0 + KM, \gamma_1 + ||\boldsymbol{y} - \boldsymbol{H}(\boldsymbol{\varepsilon}^v, \boldsymbol{\varepsilon}^r)\boldsymbol{x}||^2\right) \\ \sigma_x^2|\boldsymbol{y}, \boldsymbol{x} &\sim \mathcal{IG}\left(||\boldsymbol{x}||_0 + \beta_0, ||\boldsymbol{x}||^2 + \beta_1\right) \\ w|\boldsymbol{y}, \boldsymbol{x} &\sim \mathcal{B}e\left(||\boldsymbol{x}||_0 + 1, \bar{K}\bar{M} - ||\boldsymbol{x}||_0 + 1\right) \end{aligned}$$

where $||\boldsymbol{x}||_0$ is the number of non-zero elements in $\boldsymbol{x}$.

4.2. Sampling of $(\boldsymbol{\varepsilon}^v, \boldsymbol{\varepsilon}^r)$

The parameters $(\boldsymbol{\varepsilon}^v, \boldsymbol{\varepsilon}^r)$ are jointly sampled element-wise. Using (11),(8) and $||\boldsymbol{h}_{\bar{i}}(\varepsilon_{\bar{i}}^v, \varepsilon_{\bar{i}}^r)||^2 = 1$ we obtain

$$f(\varepsilon_{\bar{i}}^v, \varepsilon_{\bar{i}}^r|\boldsymbol{y}, \boldsymbol{\varepsilon}_{-\bar{i}}^v, \boldsymbol{\varepsilon}_{-\bar{i}}^r, \boldsymbol{x}, \sigma^2; x_{\bar{i}} = 0) = \delta(\varepsilon_{\bar{i}}^v)\delta(\varepsilon_{\bar{i}}^r) \tag{13a}$$

$$\begin{aligned} &f(\varepsilon_{\bar{i}}^v, \varepsilon_{\bar{i}}^r|\boldsymbol{y}, \boldsymbol{\varepsilon}_{-\bar{i}}^v, \boldsymbol{\varepsilon}_{-\bar{i}}^r, \boldsymbol{x}, \sigma^2; x_{\bar{i}} \neq 0) \\ &\propto \exp\left\{ \sum_{i=1}^{KM-1} \kappa_i \cos\left(2\pi \left[\frac{\varepsilon_{\bar{i}}^v}{\bar{M}} n_{va}(1+\mu k)m - k\frac{\varepsilon_{\bar{i}}^r}{\bar{K}}\right] - \phi_i\right) \right\} \end{aligned} \tag{13b}$$

knowing that $(\varepsilon_{\bar{i}}^v, \varepsilon_{\bar{i}}^r) \in [-.5, .5]^2$ and where $\kappa_i = |[\boldsymbol{z}_{\bar{i}}]_i|$, $\phi_i = \angle[\boldsymbol{z}_{\bar{i}}]_i$, with $\boldsymbol{z}_{\bar{i}} = 2\sigma^{-2} x_{\bar{i}}^* [\boldsymbol{h}_{\bar{i}}^*(0,0) \odot \boldsymbol{e}_{\bar{i}}]$.

We can see that range and velocity indices are coupled in distribution (13), contrary to that of [8]. Besides, it does not belong to any familiar class of distribution so a Metropolis-Hastings move is added to the Gibbs sampler in order to sample jointly $(\varepsilon_{\bar{i}}^v, \varepsilon_{\bar{i}}^r)$. In the MH algorithm, samples are drawn from a *proposal distribution* and accepted or rejected with a given acceptance ratio [11]. The shape of the target distribution (13) depends on the signal-to-noise ratio (SNR): for high SNR values, it is peaked around the true values of $(\varepsilon_{\bar{i}}^v, \varepsilon_{\bar{i}}^r)$, whereas it is flat in the case of low SNR values. In this paper, we employ postprocessing SNR, defined as $|x_{\bar{i}}|^2/\sigma^2$. Thus, the choice of the proposal is chosen conditionally to the SNR value: i) a uniform proposal distribution for low SNR values, $\varepsilon_{\bar{i}}^v, \varepsilon_{\bar{i}}^r \sim \mathcal{U}_{[-.5,.5]^2}$. ii) a Gaussian proposal distribution for high SNR values, $\varepsilon_{\bar{i}}^v, \varepsilon_{\bar{i}}^r \sim \mathcal{N}(\boldsymbol{\mu}_{\boldsymbol{\varepsilon}}, \boldsymbol{\Sigma}_{\boldsymbol{\varepsilon}})$.

This sampling procedure was already used in [8], but here estimation of the mean and covariance matrix of the Gaussian proposal is adapted to the case of migrating targets due to coupling of indices k and m in (13). Moreover, the sampling procedure is improved wrt that of [8] in the sense that estimation of the parameters of the proposal distribution is more accurate (as described later). This ensures better sampling of the parameters $(\boldsymbol{\varepsilon}^v, \boldsymbol{\varepsilon}^r)$, but at the cost of computational efficiency.

Estimation of $\boldsymbol{\mu}_{\boldsymbol{\varepsilon}}$ First, the mean is estimated as the values of $(\varepsilon_{\bar{i}}^v, \varepsilon_{\bar{i}}^r)$ giving the maximum of (13). To do so, (13) is reformulated as

$$\begin{aligned} &f(\varepsilon_{\bar{i}}^v, \varepsilon_{\bar{i}}^r|\boldsymbol{y}, \boldsymbol{\varepsilon}_{-\bar{i}}^v, \boldsymbol{\varepsilon}_{-\bar{i}}^r, \boldsymbol{x}, \sigma^2; x_{\bar{i}} \neq 0) \propto \mathbb{I}_{[-.5,.5]}(\varepsilon_{\bar{i}}^v)\mathbb{I}_{[-.5,.5]}(\varepsilon_{\bar{i}}^r) \\ &\exp\left\{ \mathcal{R}\text{e}\left\{ \sum_{i=1}^{KM-1} [\boldsymbol{z}_{\bar{i}}]_i \exp\left\{j2\pi\left(f_{r_{ci}} k - f_{d_{ci}}(1+\mu k)m\right)\right\} \right\} \right\} \end{aligned}$$

with $f_{rci} = \varepsilon^r_{\bar{i}}/\bar{K}$ and $f_{dci} = n_{va}\varepsilon^v_{\bar{i}}/\bar{M}$. One can recognize in this last expression the coherent integration with migration compensation of vector $\boldsymbol{z}_{\bar{i}}$ [5, p.522]. Hence, $\boldsymbol{\mu_\varepsilon}$ can be estimated as the location of the maximum of this coherent integration restricted to the domain $(\varepsilon^v_{\bar{i}}, \varepsilon^r_{\bar{i}}) \in [-.5, .5]^2$.

Estimation of $\boldsymbol{\Sigma_\varepsilon}$ Then a second-order Taylor series expansion of (13) around its peak (namely, $\boldsymbol{\mu_\varepsilon}$) is conducted and (13) is approximated by

$$\varepsilon^v_{\bar{i}}, \varepsilon^r_{\bar{i}} | \boldsymbol{y}, \boldsymbol{\varepsilon}^v_{-\bar{i}}, \boldsymbol{\varepsilon}^r_{-\bar{i}} \boldsymbol{x}, \sigma^2; x_{\bar{i}} \neq 0 \sim \mathcal{N}(\boldsymbol{\mu_\varepsilon}, \boldsymbol{\Sigma_\varepsilon}) .$$

5. EXPERIMENTAL RESULTS

In this section, we depict the results obtained with the proposed algorithm on experimental data recorded with the PARSAX radar of TU Delft [12] . The data set considered entails several echoes of vehicles on a freeway; data has been pre-whitened via some ad-hoc procedure.

It can be seen in Fig.1(a) that four targets are correctly [1] estimated by the proposed algorithm and that velocity ambiguities are mitigated. However, when using a non-robustified version of the algorithm (i.e., mismatch is considered null, Fig.1(b)) the sidelobes of targets at range bin 6/7, 12 and 14 are seen as "real" targets. Note that one target is still correctly estimated (20 m/s, range bins 3/4), probably because its mismatch with respect to the range-velocity analysis grid is low.

To finish, we depict the histogram of $(\varepsilon^v_{\bar{i}}, \varepsilon^r_{\bar{i}})|\boldsymbol{y}$ for the target at range bin 6, -14.6 m/s; it is built using samples drawn by the hybrid Gibbs sampler described in Section 4. We can see that, even with a uniform prior distribution, the empirical posterior distribution is strongly peaked around the value estimated by the SSR algorithm, namely $(.32, .36)$.

6. CONCLUSION

In this paper, we present a Bayesian sparse recovery algorithm able to mitigate velocity ambiguities in the case of off-grid range migrating targets. More precisely, this algorithm relies on a robustified sparsifying dictionary suited for range-migrating targets that possibly straddle range-velocity bins. Then, the parameters of interest are estimated thanks to a Monte-Carlo Markov chain algorithm. The proposed algorithm is successfully evaluated on experimental radar data and is proved to mitigate velocity ambiguities. In the future, the algorithm could be extended to colored noise in order to deal with diffuse clutter component.

[1] Though ground truth is unknown, true values of non-ambiguous velocities were confirmed by stationarity analysis based on two consecutive bursts of M pulses [13].

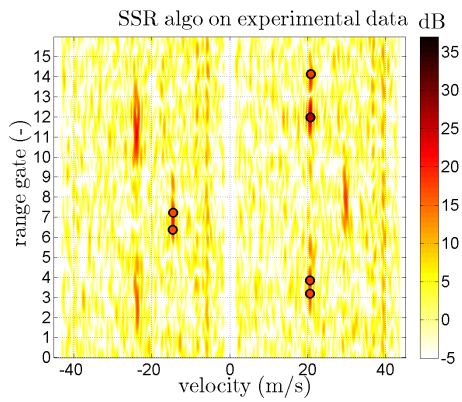

(a) Proposed algorithm

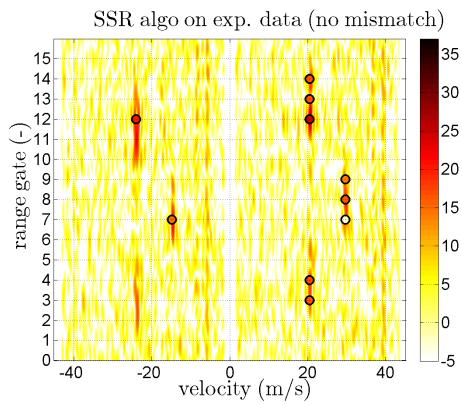

(b) No mismatch estimation

Fig. 1: Range-velocity map from PARSAX data estimated by proposed algorithm with or without mismatch estimation (circles). Coherent integration of the scene represented background. $K = 16$, $M = 64$, $f_c = 3.315$ GHz, $B = 100$ MHz, $v_a = 45$ m/s, $\sigma^2 \approx 1$. $\bar{K} = K$, $n_{va} = 2$, $\bar{M} = 2M$, $(m_{\sigma^2_x}, std_{\sigma^2_x}) = (40, 10)$ dB, $(m_{\sigma^2}, std_{\sigma^2}) = (0, 5)$ dB.

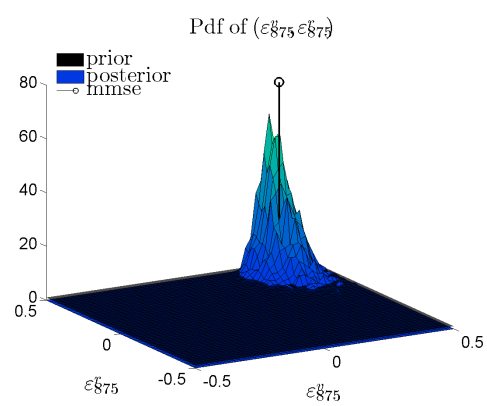

Fig. 2: Prior and empirical posterior pdf of $(\varepsilon^v_{\bar{i}}, \varepsilon^r_{\bar{i}})$ for target at range bin 6, -14.6 m/s. MMSE estimate depicted as circle.

Acknowledgement

The authors would like to thank O. Krasnov at TU Delft for kindly providing the PARSAX experimental data.

7. REFERENCES

[1] M. Richards, *Fundamentals of Radar Signal Processing*. McGraw-Hill Electronic Engineering, 2005.

[2] F. Le Chevalier, "Procédé et dispositif de détection de cibles pour radar Doppler à impulsions non ambigü à large bande," 1996, French Patent 96 08509.

[3] A. Farina and F. A. Studer, "Detection with high resoluton radar: great promise, big challenge," *Microwave Journal*, vol. 34, no. 5, pp. 223–273, May 1991.

[4] J. Tsao and B. D. Steinberg, "Reduction of sidelobe and speckle artifacts in microwave imaging: the CLEAN technique." *IEEE Transactions on Antennas and Propagation*, vol. 36, no. 4, pp. 543–557, 1988.

[5] W. Melvin and J. Scheer, Eds., *Principles of Modern Radar: Advanced Techniques*. Edison, NJ: Institution of Engineering and Technology, 2012.

[6] S. Bidon, J.-Y. Tourneret, L. Savy, and F. Le Chevalier, "Bayesian sparse estimation of migrating targets for wideband radar," *IEEE Trans. Aerosp. Electron. Syst.*, vol. 50, no. 2, pp. 871–886, Apr. 2014.

[7] M. Lasserre, S. Bidon, O. Besson, and F. Le Chevalier, "Bayesian sparse Fourier representation of off-grid targets with application to experimental radar data," *Signal Processing*, vol. 111, pp. 261–273, 2015.

[8] S. Bidon, M. Lasserre, O. Besson, and F. Le Chevalier, "Bayesian sparse estimation of targets with range-Doppler grid mismatch," in *Proc. of IEEE International Radar Conference*, Arlington, VA, May 2015.

[9] Y. Chi, L. Scharf, A. Pezeshki, and A. Calderbank, "Sensitivity to basis mismatch in compressed sensing," *IEEE Trans. Signal Process.*, no. 5, pp. 2182–2195, May 2011.

[10] M. Duarte and R. Baraniuk, "Spectral compressive sensing," *Appl. Comput. Harmon. Anal.*, vol. 35, pp. 111–129, 2013.

[11] C. Robert and G. Casella, *Monte Carlo Statistical Methods*. Springer, 2004.

[12] O. A. Krasnov, G. P. Babur, Z. Wang, L. P. Ligthart, and F. van der Zwan, "Basics and first experiments demonstrating isolation improvements in the agile polarimetric FM-CW radar – PARSAX," *International Journal of Microwave and Wireless Technologies*, vol. 2, pp. 419–428, 8 2010.

[13] F. Le Chevalier, O. Krasnov, F. Deudon, and S. Bidon, "Clutter suppression for moving targets detection with wideband radar," in *Proc. of European Signal Processing Conference (EUSIPCO)*, 2011, pp. 427–430.